Neuronal growth from a volume perspective

Céline Braïni, Ghislain Bugnicourt, Catherine Villard

Neuronal growth from a volume perspective

Physical Biology

OPEN ACCESS

PAPER

Neuronal growth from a volume perspective

Céline Braïni[1], Ghislain Bugnicourt[2] and Catherine Villard[1]

[1] Physico-Chimie Curie, CNRS UMR 168, Université PSL, Sorbonne Université, Paris, France
[2] Institut Néel & CNRS, Université Grenoble Alpes, France
* Author to whom any correspondence should be addressed.

E-mail: catherine.villard@curie.fr

RECEIVED
1 September 2020

REVISED
27 October 2020

ACCEPTED FOR PUBLICATION
4 November 2020

PUBLISHED
5 January 2021

Keywords: neuron, microfluidics, actin waves, growth cones, volume

Supplementary material for this article is available online

Abstract

Microfluidic-based fluorescent exclusion method allows to tackle the issue of neuronal growth from a volume perspective. Based on this technology, we studied the two main actin-rich structures accompanying the early stages of neuron development, i.e. growth cones, located at the tip of growing neuronal processes, and propagative actin waves. Our work reveals that growth cones tend to loose volume during their forward motion, as do actin waves during their journey from the cell body to the tip of neuronal processes, before the total transfer of their remaining volume to the growth cone. Actin waves seem thus to supply material to increasingly distant growth cones as neurons develop. In addition, our work may suggest the existence of a membrane recycling phenomena associated to actin waves as a pulsatile anterograde source of material and by a continuous retrograde transport.

1. Introduction

Neurons are very unique cells due to their highly extensive and ramified morphology. During development, the tip of elongating neuronal branches have to cross long distances compared to the characteristic size of a cell body [1]. Developing neurons therefore face the specific challenge of sustaining their growth over long distances. The key sub-cellular structure implied in neurite elongation is the growth cone (GC), located at the neurite tip [2].

GCs are dynamic, actin-rich membrane protrusions. They explore their environment with their characteristic hand-like shape, looking for clues to indicate the best direction for the neurite to grow and develop [2, 3]. As described in [2], they can be seen as 'vehicle' and 'navigator', their structure and molecular composition allowing them to move and choose growth directions. Interestingly, the GCs shape and dynamics vary versus time: pausing phases alternate with reactivation phases, where GCs recover their characteristic exploratory morphology [3, 4]. This suggests that the material composing an active, 'bulky', GC might not be provided continuously but rather in a pulsatile manner.

In their seminal work, Ruthel and Banker [5, 6] have reported the periodic production, at the soma level, of actin-rich structures propagating to the tip of hippocampal rodent neurons, that they named 'actin waves' (AWs). Since then, AWs have also been observed in cortical neurons [7]. AWs are membrane protrusions presenting an overall morphology similar to GCs. But contrarily to GCs whose actin-rich peripheral domain somehow caps the microtubules of its central domain (two GC's domains separated by a contractile actin arc [2]), the AW structure extends around the neurite shaft and moves on a rail of microtubules. Consistently, GCs exhibit, apart from reorientation events, a rather uniform filopodia angular distribution [8], whereas AWs filopodia are in average slightly tilted toward the shaft and distributed around an angle of 45° on each neurite side [9]. Interestingly, the overall shape of the myosin IIb distribution is quite similar in GCs and AWs, but while myosin IIb colocalizes with the actin arc in GCs, this protein is mainly found on each side of the neurite

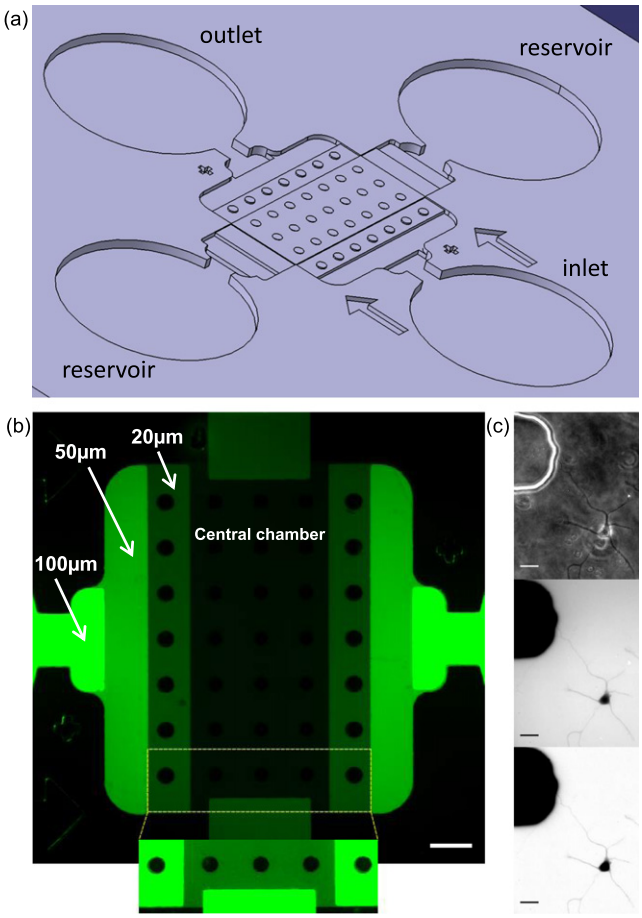

Figure 1. Microfluidic device dedicated to the study of neuronal volume by fluorescent exclusion. (a) General scheme of the device that consists in a central area containing pillars accessible through four 1.5 mm diameter inlets. More precisely 'inlet' and 'outlet' are holes dedicated to cell seeding while the 'reservoirs' contain cell medium. (b) The chamber is here filled with 10 000 MW dextran absorbing at 488 nm (1 mg ml^{-1}) to reveal the different heights (indicated in white) of this multi-compartment chamber, from the 10 μm high central chamber to the highest intermediate chamber (100 μm in height). Bottom inset: view of a part of the device using a different intensity dynamic range, revealing with higher contrast the pillars supporting the central chamber. Scale bar: 200 μm. (c) Images of a neuron located in the central chamber next to a reference pillar. The upper image shows the phase contrast whereas the middle one shows the fluorescence exclusion image and the lower one the fluorescence exclusion image after background correction. Scale bars 20 μm.

shaft at the rear of AWs [10]. In addition, an enrichment in microtubules is observed in and behind AWs, associated with a neurite enlargement [11].

Ruthel and Banker have suggested that AWs may provide a slow transport of GC material from the soma to the neurite tip at a velocity of a few μm min^{-1}. Many GC molecular constituents have indeed been identified within AWs, such as actin-associated proteins (Arp3 [7], cofilin [12], or shootin [13]) or microtubule-associated proteins (DCX [14] and more recently Ran GTPase which regulates non-centrosomal microtubule nucleation [15]). Note finally that AWs are only produced during the first stages of neurite elongation: at 5 days *in vitro* (5DIV) where the length of axons in culture can exceed one millimeter [16], they are about 3 times slower and 2 times less frequent compared to 1-2DIV [6, 7].This supports the hypothesis of the crucial role of AWs in neuronal development.

However, the exact role of AWs is still debated. If it is well admitted that AWs successively pull on the GC before merging in it, triggering its forward motion [5, 6, 11], the close amplitudes of these backward and forward motions [17] made the issue of the direct contribution of AWs into net neurite growth a subject of a recent controversy [10]. While most authors working on embryonic neurons reported that AWs induce a net neurite growth [5–7, 11, 17], the opposite result was found in a study using newborn P2–P3 rodents as a neuron source [10]. The link between AWs and GCs, the amount of material they contain and eventually exchange as a function of time and space, are therefore key points in the understanding of the modalities of neuronal growth. Supporting the early hypothesis of their 'material provider' function on a morphological basis, it was previously observed that the area of GCs increases in average by a factor $\geqslant$2 when AWs finally reach the tip [7, 10]. However, the measurement of the area only provides a partial idea of the exact magnitude of this GC refill. Both GCs and AWs being 3D structures, an estimation of the transferred volume would be more informative.

In this work, we used a method based on the imaging of the excluded volume of a cell, i.e. the fluorescence eXclusion method (FXm) [18], to access neuronal volume of immature neurons extracted from mice embryos. FXm allows long-term optical imaging without cell labeling, and provides sub-optical axial resolution defined by the maximum fluorescence intensity in the culture chamber (i.e. in a region devoid of cells) divided by the dynamic range of the camera. Different sources of noise might however degrade this ultimate resolution. We therefore used in this work a dedicated microfluidic chamber previously developed for neuronal volume imaging in which the architecture, roughness and height of the central chamber were devised to achieve the best compromise between axial resolution and technological complexity [19]. We focused on a quantitative follow-up of the volume changes versus time and space of AWs and GCs. Our results show similar spatial rate of volume loss for these two structures, possibly combined with a flow of the corresponding constituents (e.g. membrane-associated molecules) back to the soma. By counterbalancing this retrograde flow by an anterograde transport of material, AWs might in addition support a recycling phenomenon of neurite components. Overall, our study sheds a new light on the cooperation between GCs and AWs, highlighting the fundamental role of AWs in supplying material for neuronal growth, and in sustaining GC's activity over long distances.

2. Methods

2.1. Microfluidic PDMS chip

The design is presented in figure 1 and contains a 10 μm high measurement (central) chamber and three intermediate chambers of 20, 50 and 100 μm in height located between the central chamber and the inlets. The role of these intermediate chambers is to progressively reduce the light intensity coming from the inlets, which otherwise would constitute a source of light noise in the measurement chamber.

Microfluidic chips for volume measurement were prepared using polydimethylsiloxane (PDMS) mixed with its curing agent at 1:10 (Sylgard 184) and poured in an SU-8 photoresist mold as described in [19]. After removing bubbles that could interfere with our measurement using a vacuum desiccator, the mold containing PDMS is placed in an oven at 70° during 2 h. The chip is then demolded and sticked to a FluoroDish culture dish following a surface activation step provided by an oxygen plasma treatment. The devices are then immediately filled with Poly-ornithine (PLO, Sigma P4957) at 100 μg ml^{-1}. The chip is usually incubated overnight (and no less than 2 h) at room temperature (RT), then rinsed with PBS and conserved at 4 °C until the cell culture.

2.2. Neuron cell culture

We used Lifeact-GFP mice to visualize the morphology of actin-rich structures such as GCs and AWs. GFP-LifeAct hippocampal neurons were extracted from E17 mouse embryos taken out from a mother euthanized by cervical dislocation. Steps of dissection are detailed in [20].

Cells were centrifuged at 100 × g for 6 min at RT and were resuspended at 10 million cells/ml in the following culture medium: MEM containing phenol red 81.8% (LifeTech 21090-022); sodium pyruvate 100 mM 1% (LifeTech 11360-070); Glutamax 200 mM 1% (LifeTech 35050-061); horse serum 5% (LifeTech 26050088); B27 supplement 2% (LifeTech 12587-010), N2 supplement 1% (LifeTech 17502-048), gentamicin 0.2% (LifeTech 15710-049). They were then seeded in the microfluidic chip by injecting 2–3 μl of this suspension into both inlet and outlet.

2.3. Imaging

Observations were made at 1 or 2 days *in vitro* (DIV1 or DIV2), i.e. at an early stage where most cells did not display a long axon. Cells were prepared for imaging by replacing the culture medium with a similar medium but made from MEM without phenol red (LifeTech 51200-038), and to which 10 000 MW Dextran absorbing at 647 nm (LifeTech D-22914) was added (0.5 mg ml^{-1}) for volume imaging in the Cy5 channel.

Images were taken every 3 or 4 min during 10 to 24 h using an epifluorescence microscope equipped with an environmental chamber regulated at 37 °C and 5% of CO2 and a 40X, numerical aperture 0.8, dry objective. We progressively rised the exposure time to reach a 16 bit mode to be able to collect enough photons while illuminating neurons as less as possible typical range of illumination values are 10 to 30% of full power (full power : 3 W) and 4 to 30 ms of exposure time in the Cy5 channel and 17 to 100% of full power and 5 to 40 ms of exposure time in the GFP channel.

2.4. Image analysis

ROIs were manually drawn at each time point using ImageJ in the GFP (actin) channel to select areas encompassing AWs and GCs structures, as detailed in figure S1 (https://stacks.iop.org/PB/18/016007/mmedia).

We tracked the location of GCs and AWs versus time from the position of the center of mass of the intensity of the GFP (actin) fluorescence signal.

For volume measurement, we first normalized the images in the Cy5 channel using a background reduction routine [18, 19]. Raw and normalized images are presented in figure 1(c) as well as the corresponding phase image. Then we integrated the pixel intensity value in the ROIs. The last step consists in the intensity to volume conversion. The dark zone delimited by

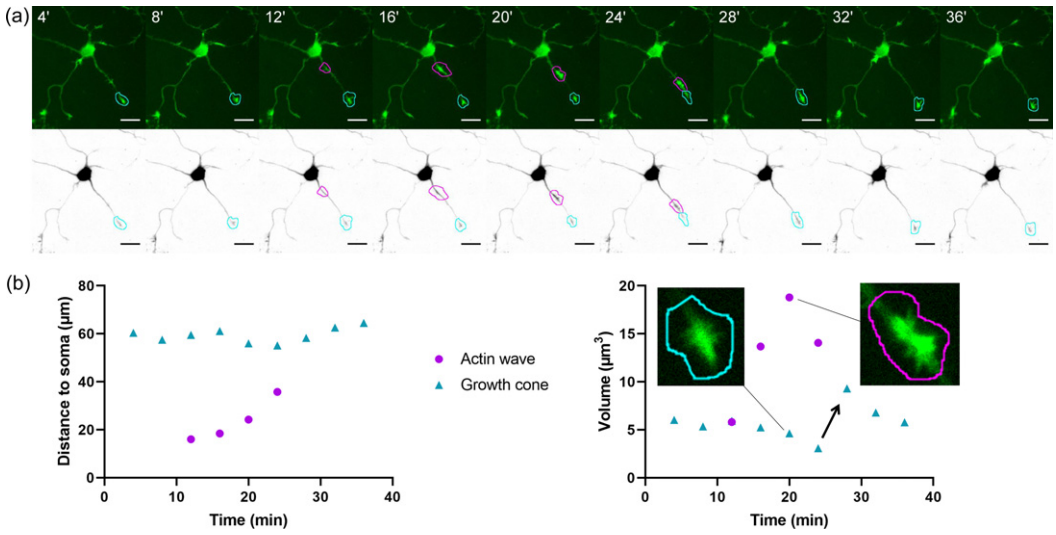

Figure 2. GC and AW position and volume versus time. (a) Neuron imaged at 2 DIV in a 10 μm high central culture chamber filled with 10 000 MW dextran absorbing at 647 nm (0.5 mg ml^{-1}). Top: GFP channel (LifeAct-GFP in green), bottom: Cy5 channel (fluorescent exclusion imaging: the intensity decreases at the cell location). Magenta lines surround an AW. Cyan lines delimit a GC. Time is indicated in minutes. Scale bars: 20 μm. (b) Graphs of the position and computed volume of the GC and AW shown in A. The gain of volume of the GC after merging of the AW is shown (arrow). Insets highlight both a GC (delimited by the blue line) and an AW (pink line) at $t = 20$.

pillars (a pillar should always be included in the imaging zone) gives the zero height reference whereas the knowledge of the precise chamber height provides the second point of the linear intensity versus height calibration [18, 19]. For more details about the intensity to volume conversion, see figure S2.

3. Results

We quantified the spatial and temporal variations of the volume of GCs and AWs in hippocampal neurons using the microfluidic chamber presented in figure 1. Note that considering the early developmental stage of neurons used in this study, we did not attempt to discriminate between axons and minor processes and considered all of them as neurites. A typical example of such analysis for one GC and one AW is given in figure 2, displaying two image sequences in both GFP and Cy5 channels [figure 2(a), see also the associated supplementary movie 1] as well as the corresponding graphs displaying the position and volume versus time of the two structures (figure 2(b)).

Several novel observations can be made from figure 2 besides the typical and expected backward then forward motion of the GC associated to the anterograde displacement and merging of the AW, respectively. Firstly, the volume follow-up of the AW shows a first increase in volume followed by a decrease. Then, at the end of the AW journey, part of its volume is transferred to the GC, making it bigger. Finally, apart from this event of volume increase, we notice a constant decrease of GC volume versus time.

From this last observation, we decided to compute the GC volume gain after AW merging to the tip, represented by the arrow on figure 2(b), versus the final AW volume measured just before the merging with the GC (figure 3(a)). We observed that the GC volume gain increases with the final volume of the AW just before merging into the GC. A linear fit of the data gives a slope of 0.67 showing that 2/3 of the AW volume that reached the tip of the neurite is transferred to the GC. To quantify further what it means in terms of volume increase for GCs, we then plotted the fold change distribution of GCs area and volume values after merging with AWs (figure 3(b)). We found a mean volume gain of a factor of 5.0. The same analysis for the GC area gives a fold change of 2.0, in agreement with previous results presented in [7, 10]. In other terms, the result we obtained in terms of volume confirm the reactivation of GCs by AWs, showing even more clearly the transfer of material between these two structures. The fold change for the volume is much higher than what would have been expected if the GC had kept its morphology in each dimension (i.e. a volume fold change of $2.0^{3/2} = 2.8$, following the size increase in each dimension of $2.0^{1/2}$). These results indicate that GCs upon AWs reactivation widen, and thicken even more.

Next, we wondered what could be the relation between the starting volume of a reactivated GC (and besides the volume of the AW which has refilled it) and the amplitude of it forward motion. To avoid any possible interference between two successive AWs (a second AW coming too soon after a first one might pull on an otherwise moving forward GC, resulting in an underestimation of the GC forward displacement), we considered AWs sufficiently distant in time to let the GC position stabilize (figure S3). Figure 3(c) shows that the higher are the AW (before merging)

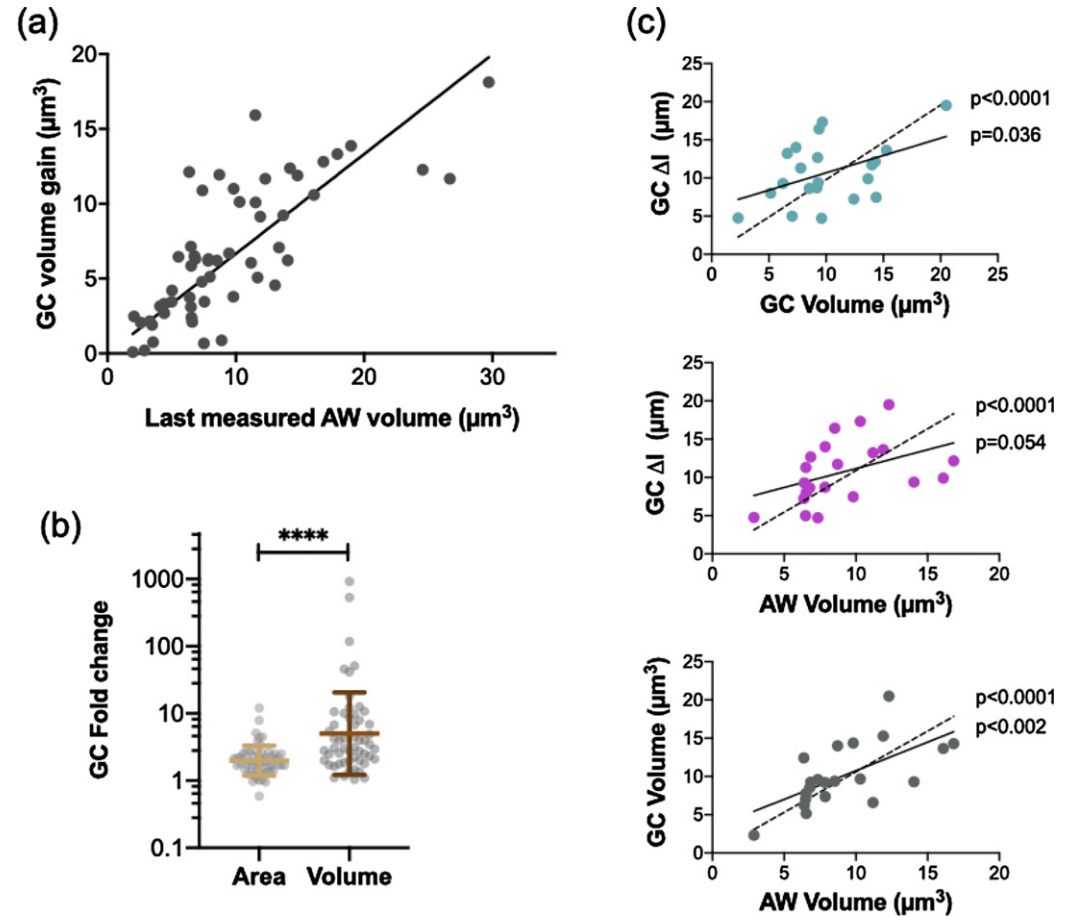

Figure 3. AWs refill GCs in volume. (a) Volume transfer between AWs and GCs and linear fit passing through origin (slope 0.67 and confidence range [0.60–0.74], $p < 0.0001$), $n = 55$, 22 neurons. (b) GC area and volume fold change calculated by dividing each GC area or volume value after merging with the AW by its value just before the merging. The horizontal bars represent the geometric mean (GM) and the geometric standard deviation factor (GSD). Area (GM, GSD): (2.0, 1.7), volume (GM, GSD): (5.0, 4.1), $n = 55$, 22 neurons. (c) GC forward motion Δl as a function of the GC volume measured just after AW merging into the tip (top graph), and as a function of the AW volume just before merging (middle graph). The bottom graph expresses the significant dependance between GC's (after merging) and AW's (before merging) volumes. Dashed line: linear fit going through origin, solid line: best linear fit. The p values of these linear fits are indicated on the graphs. $n = 21$, 9 neurons.

and GC (after merging) volumes, the farther goes the GC.

Next, we turned out our attention to the volume dynamics of AWs, following the intriguing observation made from figure 2 of an increase followed by a decrease of the AW volume during its journey from the soma to the tip. Computing a large number of AWs, and taking into account only cases where the whole volume change could be observed on 4 or more time points, we found that a volume decrease was observed in 83% of the cases (42 AWs observed from 17 cells). Interestingly, 60% of these AWs (i.e. 50% of all measured AWs) present a first increase of volume near the soma. Figure 4(a) displays these AW volume variations versus the distance to the soma. After normalizing the AW volume to its maximal value, and the distance to the soma to the distance at which the AW displays its maximal volume, the phase of volume decrease of a set of 35 AWs collapses rather well on a master linear variation. Interestingly, the rate of volume loss seems to scale with the maximum or the initial volume of AWs, as shown in figure 4(b).

From figure 2, we also observed that AWs were not the only structure to lose volume versus distance: GCs displayed a similar behavior. The velocity of these two structures being very different, typically a few μm min^{-1} for AWs and less than a μm min^{-1} for GCs, we decided to compare the dynamic of volume loss versus distance and time of both AWs and GCs (figure 5). In this analysis, only periods of forward motion of the GCs were taken into account. We first observed that AWs are losing volume in time faster than GCs (mean $\pm$ SD: 1.1 ± 0.3 μm^3 min^{-1} vs 0.3 ± 0.2 μm^3 min^{-1}). Very interestingly, the ratio between these values is very similar to the ratio between the mean velocities of the two structures (2.5 μm min^{-1} for AWs and 0.7 μm min^{-1} for GCs). Expectedly, abolishing time and looking at the volume loss versus distance, we found that AWs and GCs lose volume at a similar rate of 0.5–0.6 μm^3 μm^{-1}.

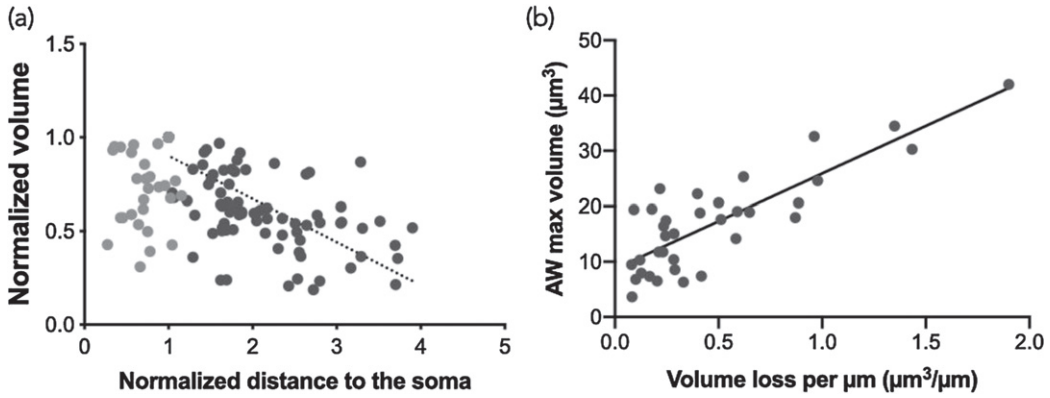

Figure 4. AWs volume dynamic. (a) Normalized (to its maximal value) volume of all AWs measured along neuronal extensions. This graph shows two phases according to the distance to the cell body (normalized to its value at the maximal AW volume): the volume gain (light gray) and the volume loss (dark gray). Dotted line: linear fit of the volume loss data ($p < 0.0001$). $n = 35$, 15 cells. (b) AW max volume versus the volume loss per distance and linear fit: slope 17.2 μm, $p < 0.0001$, $n = 35$, 15 cells.

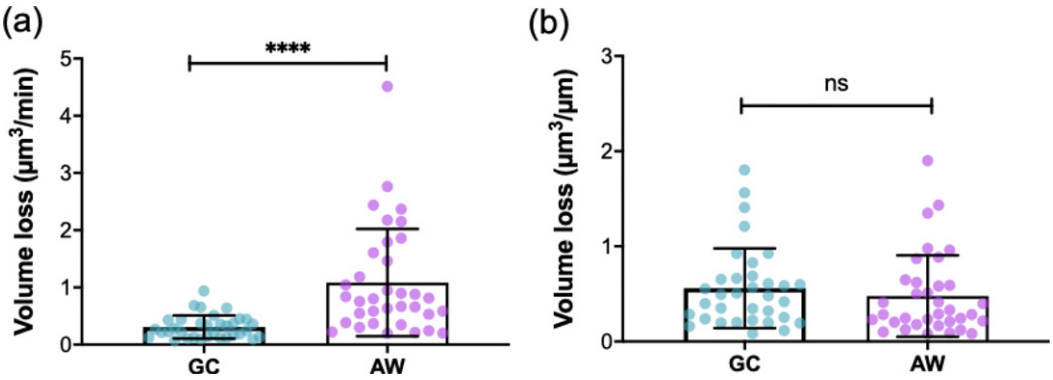

Figure 5. Volume loss during forward motion of both structures. (a) Distribution of the slopes of the linear fits of volume loss versus time for GCs (mean ± SD: 0.3 ± 0.2 μm^3 μm^{-1}, $n = 34$, 15 cells) and AWs (mean ± SD: 1.1 ± 0.3 μm^3 μm^{-1}, $n = 35$, 15 cells), $p < 0.0001$. (b) Distribution of the slopes of the linear fits of volume loss versus distance for GCs (mean ± SEM: 0.56 ± 0.07 μm^3 μm^{-1}, $n = 34$, 15 cells) and AWs (mean: 0.48 ± 0.07 μm^3 μm^{-1}, $n = 35$, 15 cells), ns: non significant.

4. Discussion

In this work, we have shown that GCs tend to exhaust themselves naturally versus time and distance as they move forward. They thus need to be periodically refueled until they reach their final target, allowing the establishment of mature neuronal networks. It is well established that an intense and fast (a few μm s^{-1}) trafficking of molecules and various organelles (vesicles, mitochondria) sustain neuronal growth [21]. In this work, we explored how the slow transport provided by AWs contributes to GC activity. We showed the existence of a massive transfer of volume between AWs and GCs, revealed by the slope of 0.67 between the volume of the AWs before merging into the GC and the GC after merging. Let us note that, due to the 3 to 4 min time step between each image in our timelapse experiments, the position of an AW before merging can be as far as 10 μm from the tip. Considering our finding that AWs also lose volume during their forward motion, we inevitably end with an over-estimation of the final AW volume. This might explain why we do not observe a linear fit with a slope closer to 1. We also found a clear positive dependence between the volume of a GC and its forward motion. This is an important result, highlighting the importance of GC's initial volume for its following forward exploratory activity, and thereby the crucial role of AWs for periodic GC refueling.

Our results raises the question of the destination of the material leaking from both AWs and GCs, plausibly assuming that the volume loss we observe involves e.g. membrane and cytosol loss. As the activity of these two actin-rich structures occurs during neuronal growth, one possible answer would be that the material they lose along their way forward is used to built a new neurite portion at the tip. We thus measured the volume per unit of length of a neurite and found a value of 0.26 ± 0.02 (Mean ± SEM) μm^3 μm^{-1}, (see supplementary figure S4), about twice below the value of 0.56 μm^3 μm^{-1} associated to GC volume loss. GCs thus lose about 2 times more volume per micron that what is necessary to extend the length of a neurite by one micron. The remaining extra-volume might eventually serve to build the

transient enlargement of the neurite upstream of the AW, as reported in the work of Winans *et al* ([11]), by bringing some extra membrane material. But this remains very speculative at this stage.

Overall, the question of the destination of the lost volume, and beyond that of its composition, are clearly out of the scope of this work. However, as preliminary data, we observed that beads attached on a neurite surface where constantly brought back to the soma at velocities in the range of a few μm min^{-1}, thus rather similar to the velocities of AWs (see supplementary figure S5). Similarly to what has been observed for fast transport [21], it seems thus that the slow transport of material is also bidirectional. In this frame, AWs would provide a pulsatile anterograde mode of transport, while the retrograde flow would seem conversely constant, concerning both AWs and GCs (consistently with our observation that the rate of volume loss versus distance of AWs and GCs is similar, although their velocities differ). In addition, let us note that GCs are losing volume in both forward and backward motions, supporting the hypothesis of a robust and constant material retrograde transport, independent of the intrinsic behavior of the structures it comes from (see supplementary figure S6). Interestingly, our observations are consistent with the conclusions of the work of Dai and Sheetz [22]. These authors demonstrated that the axonal membrane of chick neurons flows from the tip to the soma at a speed of a few μm min^{-1}, and attributed this flow to a gradient of membrane tension, with the lowest tension at the GC due to the insertion of new membrane at this growing site. These authors suggested that this phenomena may allow a recycling of the composition of the membrane along the entire axon. In the case of mammalian neurons like the hippocampal neurons used in this study, the situation is a bit more complex from the presence of AWs, which are also participating to neurite tension. However, by providing a pulsatile source of extra-membrane material at the tip, they might be a source of a pulsatile gradient of membrane tension powering the flow that would deprive both themselves and GC from their content.

5. Conclusion

The volume study of neuronal growth we have used in this work shows that AWs constitute a source of material able to periodically reactivate GCs. They also transfer to GCs much more material that is necessary for neurite elongation. This balance sheet, and the fact that both AWs and GCs lose volume over time and space, suggest the existence of a retrograde flow of material, whose existence and role should be confirmed, but which might serve to adjust in a typically tens of minutes to hours scale the properties of the huge membrane surface (in particular compared with the volume enclosed by neurites) of growing neurons. Finally, while our work does not exclude the fact that AWs may directly trigger net neurite growth, it unambiguously supports the idea that AWs, among other possible roles, supply materials to increasingly distant GCs, thereby contributing to the establishment of neuronal extension over long distances.

Acknowledgments

This work was supported by the European Research Council Advanced Grant 321107 'CellO' and by the HoliFAB project funded by the European Union's Horizon 2020 research and innovation program (grant agreement No 760927). This work has also received the support of Institut Pierre-Gilles de Gennes-IPGG (Equipement d'Excellence, 'Investissements d'avenir', program ANR-10-EQPX-34). We also thank the Grenoble Institut des Neurosciences for support during the PhD of Ghislain Bugnicourt.

ORCID iDs

Catherine Villard https://orcid.org/0000-0002-5379-1067

References

[1] Harris J M, Wang A Y-D, Boulanger-Weill J, Santoriello C, Foianini S, Lichtman J W, Zon L I and Arlotta P 2020 Long-range optogenetic control of axon guidance overcomes developmental boundaries and defects *Dev. Cell* **53** 577–88

[2] Lowery L A and van Vactor D 2009 The trip of the tip: understanding the growth cone machinery *Nat. Rev. Mol. Cell Biol.* **10** 332–43

[3] Kalil K and Dent E W 2005 Touch and go: guidance cues signal to the growth cone cytoskeleton *Curr. Opin. Neurobiol.* **15** 521–6

[4] Knobel K M, Jorgensen E M and Bastiani M J 1999 Growth cones stall and collapse during axon outgrowth in *Caenorhabditis elegans Development* **126(20)** 4489–98 PMID: 10498684

[5] Ruthel G and Banker G 1998 Actin-dependent anterograde movement of growth-cone-like structures along growing hippocampal axons: a novel form of axonal transport? *Cell Motil. Cytoskelet.* **40** 160–73

[6] Ruthel G and Banker G 1999 Role of moving growth cone-like 'wave' structures in the outgrowth of cultured hippocampal axons and dendrites *J. Neurobiol.* **39** 97–106

[7] Flynn K C, Pak C W, Shaw A E, Bradke F and Bamburg J R 2009 Growth cone-like waves transport actin and promote axonogenesis and neurite branching *Dev. Neurobiol.* **69** 761–79

[8] Buettner H M, Pittman R N and Ivins J K 1994 A model of neurite extension across regions of nonpermissive substrate: simulations based on experimental measurement of growth cone motility and filopodial dynamics *Dev. Biol.* **163** 407–22

[9] Katsuno H, Toriyama M, Hosokawa Y, Mizuno K, Ikeda K, Sakumura Y and Inagaki N 2015 Actin migration driven by directional assembly and disassembly of membrane-anchored actin filaments *Cell Rep.* **12** 648–60

[10] Mortal S, Iseppon F, Perissinotto A, D'Este E, Cojoc D, Napolitano L M R and Torre V 2017 Actin waves do not

boost neurite outgrowth in the early stages of neuron maturation *Front. Cell. Neurosci.* **11** 402
[11] Winans A M, Collins S R and Meyer T 2016 Waves of actin and microtubule polymerization drive microtubule-based transport and neurite growth before single axon formation *Elife* **5** e12387
[12] Tilve S, Difato F and Chieregatti E 2015 Cofilin 1 activation prevents the defects in axon elongation and guidance induced by extracellular alpha-synuclein *Sci. Rep.* **5** 16524
[13] Toriyama M, Shimada T, Kim K B, Mitsuba M, Nomura E, Katsuta K, Sakumura Y, Roepstorff P and Inagaki N 2006 Shootin1: a protein involved in the organization of an asymmetric signal for neuronal polarization *J. Cell Biol.* **175** 147–57
[14] Tint I, Jean D, Baas P W and Black M M 2009 Doublecortin associates with microtubules preferentially in regions of the axon displaying actin-rich protrusive structures *J. Neurosci.* **29** 10995–1010
[15] Huang Y A, Hsu C H, Chiu H C, Ho C T, Lo W L and Hwang E 2019 Ran GTPase regulates non-centrosomal microtubule nucleation and is transported by actin waves towards the neurite tip (bioRxiv:684720)
[16] Ahnert-Hilger G, Höltje M, Grosse G, Pickert G, Mucke C, Nixdorf-Bergweiler B, Boquet P, Hofmann F and Just I 2004 Differential effects of Rho GTPases on axonal and dendritic development in hippocampal neurones *J. Neurochem.* **90** 9–18
[17] Tomba C, Braïni C, Bugnicourt G, Cohen F, Friedrich B M, Gov N S and Villard C 2017 Geometrical determinants of neuronal actin waves *Front. Cell. Neurosci.* **11** 86
[18] Cadart C, Zlotek-Zlotkiewicz E, Venkova L, Thouvenin O, Racine V, Le Berre M, Monnier S and Piel M 2017 Fluorescence exclusion measurement of volume in live cells *Methods Cell Biol.* **139** 103–20
[19] Braïni C, Mottolese A, Ferrante I, Monnier S and Villard C 2018 High-resolution volume imaging of neurons by the use of fluorescence exclusion method and dedicated microfluidic devices *JoVE* **133**
[20] Fath T, Ke Y D, Gunning P, Götz J and Ittner L M 2008 Primary support cultures of hippocampal and substantia nigra neurons *Nat. Protoc.* **4** 78–85
[21] Moutaux E, Christaller W, Scaramuzzino C, Genoux A, Charlot B, Cazorla M and Saudou F 2018 Neuronal network maturation differently affects secretory vesicles and mitochondria transport in axons *Sci. Rep.* **8** 1–14
[22] Dai J and Sheetz M P 1995 Axon membrane flows from the growth cone to the cell body *Cell* **83** 693–70